

1 **Assessing the extreme risk of coastal inundation due to climate**
2 **change: A case study of Rongcheng, China**

3 Aiqing Feng^{1,2}, Jiangbo Gao¹, Shaohong Wu^{1*}, Yanzhong Li^{2,3}, Xiliu Yue^{1,2}

4 ¹Key Laboratory of Land Surface Pattern and Simulation, Institute of Geographical Sciences and Natural Resources
5 Research, Chinese Academy of Sciences, Beijing 100101, China;

6 ²University of Chinese Academy of Sciences, Beijing 100049, China;

7 ³Key Laboratory of Water Cycle and Related Land Surface Processes, Institute of Geographical Sciences and Natural
8 Resources Research, Chinese Academy of Sciences, Beijing 100101, China.

9

10 *Corresponding author: Shaohong Wu

11 E-mail: wush@igsnr.ac.cn

12

13 **Abstract:** Extreme water levels, caused by the joint occurrence of storm surges and high tides,
14 always lead to super floods along coastlines. Given the ongoing climate change, this study explored
15 the risk of future sea-level rise on the extreme inundation by combining P-III model and losses
16 assessment model. Taking Rongcheng as a case study, the integrated risk of extreme water levels
17 was assessed for 2050 and 2100 under three Representative Concentration Pathways (RCP)
18 scenarios of 2.6, 4.5, and 8.5. Results indicated that the increase in total direct losses would reach
19 an average of 60% in 2100 as a 0.82 m sea-level rise under RCP 8.5. In addition, affected population
20 would be increased by 4.95% to 13.87% and GDP (Gross Domestic Product) would be increased by
21 3.66% to 10.95% in 2050 while the augment of affected population and GDP in 2100 would be as
22 twice as in 2050. Residential land and farmland would be under greater flooding risk in terms of the
23 higher exposure and losses than other land-use types. Moreover, this study indicated that sea-level
24 rise shortened the recurrence period of extreme water levels significantly and extreme events would
25 become common. Consequently, the increase in frequency and possible losses of extreme flood
26 events suggested that sea-level rise was very likely to exacerbate the extreme risk of coastal zone in
27 future.

28 **Keywords:** sea-level rise; inundation risk; extreme water level; expected direct losses; affected
29 population and GDP; recurrence period.

30

31 **1 Introduction**

32 Coastal inundation is predominantly caused by extreme water levels when storm surges are
33 concurrent with astronomical high tides (e.g. Pugh, 2004; Quinn et al., 2014). Statistically, the
34 extreme flood events were occurred frequently and caused huge devastation (Trenberth et al., 2015).
35 Recent research indicated that sea-level rise, with global mean rates of 1.6 to 1.9 mm yr⁻¹ over the
36 past 100 years (Holgate, 2007; Church and White, 2011; Ray and Douglas, 2011), had been strongly
37 driving the floods (Winsemius et al., 2016). Global mean sea-level ^{is} was expected to rise more than
38 1 m by the end of this century (Levermann et al., 2013; Dutton et al., 2015), even if global warming
39 can be controlled within 2°C. Thus, coupled with continuous sea-level rise induced to climate
40 change, the future coastal inundation risk in terms of hazards and possible losses should be paid

prefer
indicates
idem

7

41 attention to disaster mitigation.

42 Projections for extreme water levels are indispensable for inundation risk assessment. Most
43 researches to date have focused on the coastal flooding caused by storm surges (e.g. Bhuiyan and
44 Dutta, 2011; Klerk et al., 2015). At present, exceedance probabilities of current extreme water level,
45 induced by tropical and extra-tropical storm surges, have been estimated (Haigh et al., 2014a, b).

why
this
sentence?

46 However, on account of the sea-level rise, coastal flooding disasters would become more serious
47 (Feng et al., 2016) and 85% of global deltas experienced severe flooding in recent decades (Syvitski
48 et al., 2009). Feng and Tsimplis (2014) showed that extreme water level around the Chinese

→ 1 / in how many year

49 coastline was increased by 2.0 mm to 14.1 mm yr⁻¹ from 1954 to 2012. Based on an ensemble of
50 projection to global inundation risk, it argued that the frequency of flooding in Southeast Asia is

relative SLR?

51 likely to increase substantially (Hirabayashi et al., 2013). By 2030, the portion of global urban land
52 exposed to the high-frequency flooding would be increased to 40% from a 30% level in 2000

once every year?

X

53 (Gunalp et al., 2015). Conservative projections suggested that over a half of global delta surface
54 areas would be inundated as a result of sea-level rise by 2100 (Syvitski et al., 2009).

55 The impacts of coastal flooding on social economies were considered and some methods were
56 established to estimate the possible losses (e.g. Yang et al., 2016). With the socio-economic
57 development, the large aggregations of coastal population and assets would lead to the increase
58 exposed to inundation in future (Mokrech et al., 2012; Strauss et al., 2012; Alfieri et al., 2015).

what are these

59 Without adaptation, by 2100, 0.2% to 4.6% of the global population would be at risk of flooding,
60 and expected annual GDP losses would be 0.3% to 9.3% (Hinkel et al., 2014). In particular,

→ very
low
number

61 urbanization of China was rapidly fast in the world and many low-lying coastal cities were
62 confronted with high probabilities of flooding (Nicholls and Cazenave, 2010). More than 30% of
63 the China's coast was assessed as 'high vulnerability' according the research of Yin et al., (2012),

?

64 and the population numbers exposed to flooding risk were the highest in the world (Neumann et al.,
65 2015). A number of China's cities including Guangzhou, Shenzhen, and Tianjin were in the top 20
66 global cities in terms of their exposure to 100-year inundation risk and huge average annual losses
67 because of water levels rising (Hallegatte et al., 2013).

68 Distinguishing the risk of extreme floods considering sea-level rise caused by climate change
69 is vital for disaster mitigation and adaptation on a large time scale. In this study, the flooding from
70 extreme water levels was simulated by a combination of storm surges, astronomical high tides, and

?

71 sea-level rise heights under different RCP scenarios. Using Rongcheng City as a case study, a
72 comprehensive multi-dimensional analysis was presented to assess the inundation risk based on two
73 time scales of 2050 and 2100, and three RCP scenarios of 2.6, 4.5, and 8.5. The main objectives are
74 to (1) investigate the expansion of the inundated area and the increase in expected direct losses; (2)
75 analyze the effect of sea-level rise on population and GDP; and (3) reveal the future hazard change
76 of extreme water levels by the probability of occurrence.

77 **2 Data and methodology**

78 **2.1 Study area**

79 Rongcheng City, located at the tip of the Shandong Peninsula, China, is surrounded on three sides
80 by 500 km of Yellow Sea coastline (Fig. 1). This city has low-elevation and flat topography and
81 covers an area of more than 1,500 km². Its population of 0.67 million people and GDP of \$12.31
82 billion make it become one of the top one hundred counties in China. Rongcheng experiences a
83 monsoonal climate at medium latitudes with an average annual rainfall of 757 mm and a temperature
84 of 11.7°C for nearly 50 years (data from <http://data.cma.cn/>). It is also in a critical geographical
85 position for trade exchange and the modern economy facing Korea across the Yellow Sea.
86 Substantial additional capital investment is expected in this region because the Shandong Peninsula
87 National High-tech Zone has been approved as a part of the National Independent Innovation
88 Demonstration Zone by the China's State Council in 2016 (<http://www.gov.cn/>). A inundation risk
89 assessment for Rongcheng City is urgent to its long-term development, especially under the situation
90 of sea-level uptrend due to climate change.

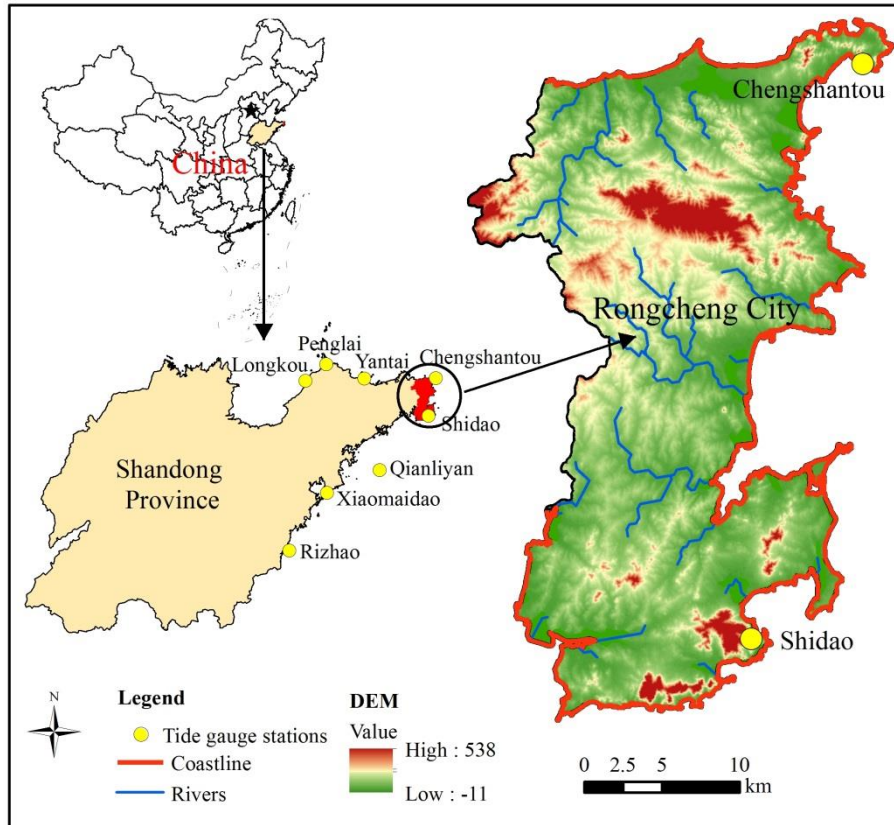


Fig. 1 Map to show the geographic locations of Rongcheng City and main tidal gauge stations

+ land use map

2.2 Assessment process and dataset

The assessment process of inundation risk followed three steps. First, extreme water levels were calculated using storm surge data, astronomical high tides, and sea-level rise heights by the method of Pearson Type III (P-III). Second, the inundated area and depth were identified by the flood model (the four nearest neighbors algorithm) using the data of extreme water levels which resulted from the first step and the Digital Elevation Model (DEM). Third, inundation risk was assessed by direct losses model and recurrence period change. The dataset was summarized in Table 1.

No subsidence of land expected?
 Change in socio-economy in coming
 50 years?

Table 1 Dataset of extreme risk assessment including hydrological, geographical, and statistical inputs

Data type	Content	Description	Source
Hydrological data	Sea-level rise	Global mean sea-level rise in 2050 and 2100 under RCPs 2.6, 4.5, 6.0, and 8.5. All scaled with two degrees (low vs. high)	IPCC (2013)
	Storm surge	Return periods of storm surges were obtained using the P-III model and historical data from 1967 to 2013	Tidal gauge stations, National State Oceanic Administration
	Astronomical high tide	Predicted using harmonic tide models based on measured data (Wu et al. 2016)	Tidal gauge stations, National State Oceanic Administration
Geographical data	1:10,000 digital topographic maps	A 10 m × 10 m DEM was built using elevation points and contour lines in ArcGIS	Bureau of Land Management
	Land-use maps	High precision grid data at a 30 m scale were used to characterize the land-use types in flooded area and calculate direct damage <i>name of map or plan</i>	Institute of Geographical Sciences and Natural Resources Research, Chinese Academy of Sciences (IGSNRR, CAS)
	Spatial distribution of GDP and population	1 km × 1 km grid data according to statistics from 2010	http://www.resdc.cn/
Statistical data	Vulnerability curves and estimated loss values for different land-use types. Abbreviations: y, loss rate (%); x, flood depth (m); V, loss values (\$/m ²).	Residential land, $y=16.682x$, $R^2=0.6359$, $V=307.69$; Farmland, $y=49.837x$, $R^2=0.4246$, $V=0.77$; Grassland and woodland, $y=36.304x$, $R^2=0.9113$, $V=12.31$; Unused land and water regions, $y=0$, $V=0$.	(Yin, 2011)

107

108 **2.3 Construction of the cumulative probability distribution of extreme water levels**

define extreme

*from data analysis!
Not constructed*

109 Extreme water level is a compound event caused by storm surges and astronomical high tides while
 110 sea-level rise also contributes to extreme water levels under global climate change. Therefore, in
 111 this study, the current extreme water levels (CEWLs) and future extreme water levels were
 112 constructed. The latter was a combination of CEWLs and projected heights of sea-level rise under
 113 different RCP scenarios and was defined as the scenario extreme water levels (SEWLs). The
 114 cumulative probability distribution curves of CEWLs and SEWLs were refitted using a P-III model
 115 as the Equation (1). The details of this method were shown as Wu et al., (2016).

116
$$f(x) = \frac{\beta^\alpha}{\Gamma(\alpha)} \int_{x_p}^{\infty} (x - \alpha_0)^{\alpha-1} e^{-\beta(x-\alpha_0)} \quad (1)$$

117 In this expression, α , β , and α_0 are the shape, scale, and location parameters, respectively; x is
118 the annual maximum values for water levels; p is the probability of occurrence.

$$119 \quad CEWL = ST + AHT \quad (2)$$

120 where ST is storm surge and AHT is astronomical high tide;

$$121 \quad SEWL = CEWL + SLR \quad (3)$$

122 where SLR is the predicted height of sea-level rise in the future;

$$123 \quad T = 1/p \quad (4)$$

124 where T stands for the recurrence period of extreme water level and the T -year recurrence level
125 means that an event of extreme water level has a $1/T$ probability of occurrence in any given year
126 (Cooley et al., 2007).

127 Because of the uncertain impacts of sea-level-rise on storm surges, the statistical probabilities
128 of storm surge in this model were assumed to be unchanged in future (e.g. Hunter, 2012; Kopp et
129 al., 2013; Little et al., 2015). The extreme water levels were mainly constructed by historical records
130 of Chengshantou and Shidao tidal stations located in Rongcheng City (Fig. S1 in Supplementary
131 data). In order to reduce the error caused by the spatial distribution of extreme water levels, recorded
132 data of the surrounding six tidal stations (including Longkou, Penglai, Yantai, Qianliyan,
133 Xiaomaidao, and Rizhao) on Shandong Peninsula were still calculated using the inverse-distance-
134 weighted (IDW) technique in ArcGIS software.

135 2.4 Identification of flooding

136 Inundated area was extracted from the flood model using the four nearest neighbors algorithm based
137 on high-resolution DEM (10 m \times 10 m) and extreme water level layers (10 m \times 10 m cells generated
138 in ArcGIS). Flooding criteria were that the extreme water level of layer cells must be greater than
139 or equal to the elevation of DEM and inundated cells must be connected to the coast individually
140 (Xu et al., 2016). The impacts of the elevations of urban landscapes and other buildings on flooding
141 process were not considered in this study. In this section, inundated area and depth could be
142 computed.

143 2.5 Inundation risk assessment

144 Expected direct losses were calculated using inundated area, inundated depth, vulnerability curves,
145 and loss values for each land-use type. The land-use map of 30 m resolution was resampled to 10 m

How large were differences between 2 stations, and six stations?

miss recurrence of flood depth 1/1 to 1/100 years

146 cells using the raster processing tool in ArcGIS in order to match inundated cells. The assessment
147 model for expected direct losses is:

$$148 \quad EDL = \sum_i A \times h \times r \times V \quad (5)$$

149 where EDL stands for the expected direct losses of extreme floods; i denotes land-use type
150 including residential land, farmland, woodland, grassland, and unused land; A denotes inundated
151 area; h stands for flood depth; r stands for loss rate (vulnerability curves); and V stands for the per-
152 unit loss value (\$/m²).

↳ include curves in the paper

153 The amounts of affected population and GDP were estimated based on the grid distribution
154 data of population and GDP (published in China 2010 at a resolution of 1 km, <http://www.resdc.cn/>).
155 Land-use cover change and socio-economic development were not considered in future (Hallegatte
156 et al., 2013; Hinkel et al., 2014; Muis et al., 2015).

Need more information on how to get 1/1000 flood from short data series

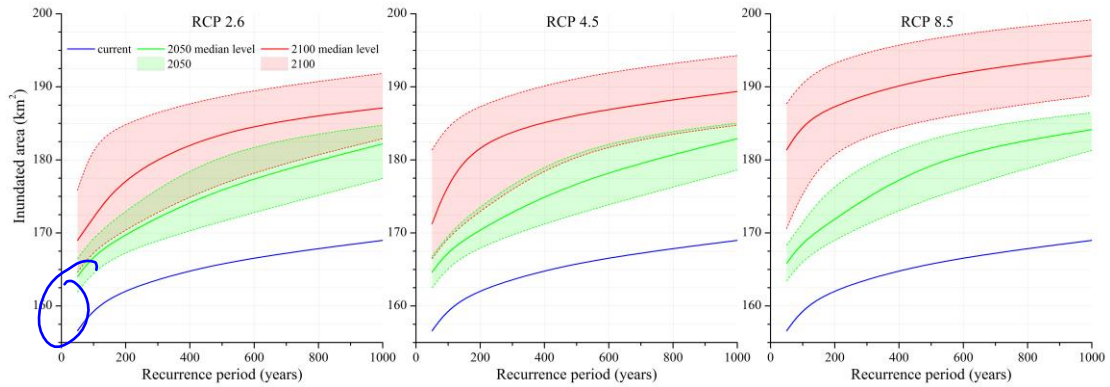
157 **3 Results and analysis**

158 **3.1 Inundated area**

159 In the absence of adaptation, the areas inundated by CEWLs and SEWLs are shown as Fig. 2. At
160 the present stage, inundated areas range from 156.60 km² to 168.8 km² when Rongcheng City
161 encounters extreme water levels. However, an expanding trend in inundated area is inevitable
162 because of future sea-level rise; in this analysis, the smallest increase in inundated area would be
163 seen under RCP 2.6 while the largest would be seen under RCP 8.5 while it would be enlarged
164 significantly by 2100 compared to 2050 as sea-level rise continues. The extreme scenario, under
165 RCP 8.5, predicts that the total area where were threatened by flooding ranges from 168.35 km² to
166 186.46 km² in 2050, and that it may be between 187.72 km² and 199.18 km² by 2100. According to
167 this projection, the maximum area is around 13% by the end of the century. At high degree for each
168 RCP scenario, inundated area increases by 2100 is likely to range from 14.21% to 19.54% given a
169 100-year recurrence. Summary statistics of future inundated area increase for 50 to 1,000-year
170 recurrence periods are presented in Table S1(a).

171

why no data on 1/1 to 1/50 recurrence?



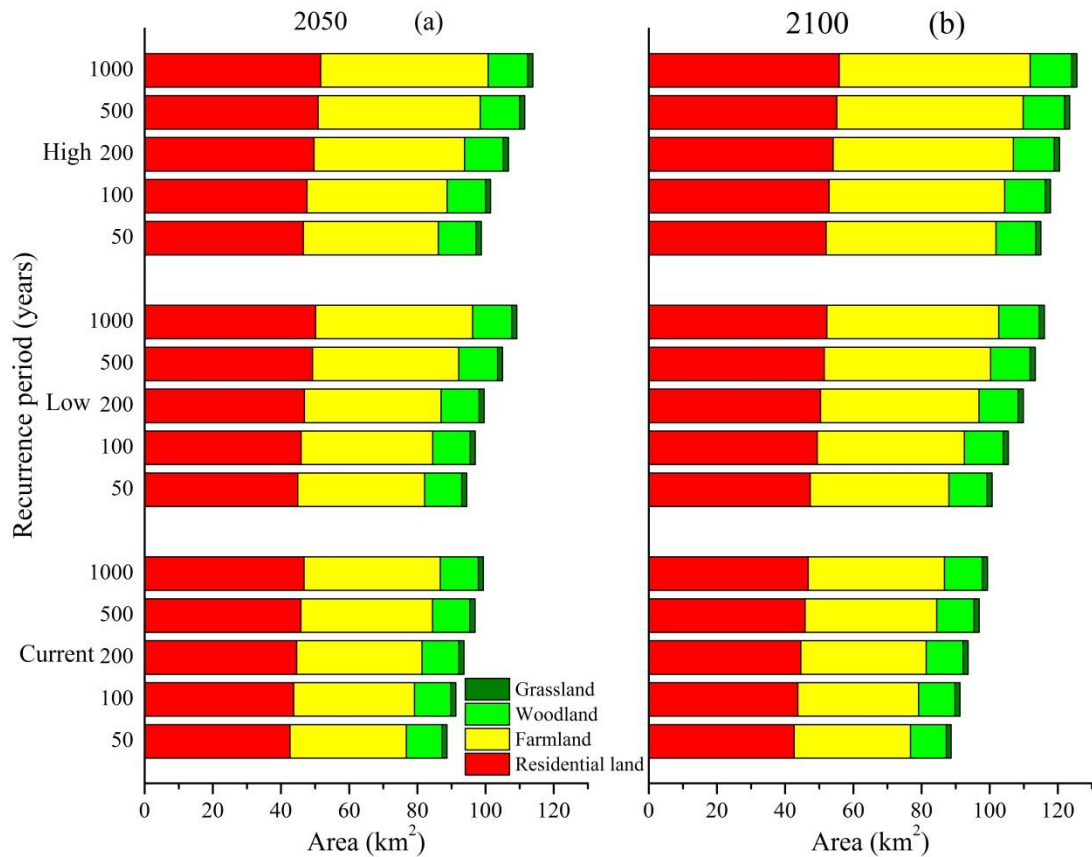
172

173 **Fig. 2** Inundated areas under different RCP scenarios for 2050 and 2100. The blue solid line denotes the inundated
174 area curve as it changes with CEWLs, while the areas outlined by green and red stippled lines denote the extent of
175 inundated areas projected on the basis of SEWLs under low and high degree RCP scenarios for 2050 and 2100,
176 respectively. The green and red solid lines denote the median degree for each RCP scenario. Similarly, the
177 explanations are used for Fig. 4 and 5.

178

179 Land-use types of residential land, farmland, woodland and grassland are involved in the
180 estimation of total inundated area while the water bodies and unused land could be ignored in this
181 study. Thus, summarizing the inundated data, the total inundated land-use areas under RCP 8.5 are
182 shown in Fig. 3. Results show that residential land and farmland are more exposed to extreme water
183 levels than woodland and grassland. Indeed, when Rongcheng City is currently subjected by
184 extreme flooding, ~~42.63 km²~~ to ~~46.77 km²~~ of residential land and ~~34.15 km²~~ to ~~39.97 km²~~ of farmland
185 would be affected, based on 50 to 1000-year recurrence periods, respectively. Given a high degree
186 RCP 8.5 scenario, inundated areas of residential land and farmland would increase to 47.61 km² and
187 41.13 km² in 2050, and to 52.88 km² and 51.47 km² in 2100, respectively. More seriously, combined
188 areas of residential land and farmland exposed to flooding would rise to around 50 km² in 2050 and
189 56 km² in 2100, respectively. The flood map (Fig. S2) shows the extension of inundated area by
190 2050 and 2100 given a 100-year recurrence period.

191



192

193

Fig. 3 Predicted inundated areas broken down by different land-use types given 50 to 1,000-year recurrence periods in 2050 (a) and 2100 (b). RCP 8.5 is taken as an example in this paper and the inundated areas of different land-use types under RCP 2.6 and 4.5 are similar.

195

196

197 3.2 Expected direct flood losses

198

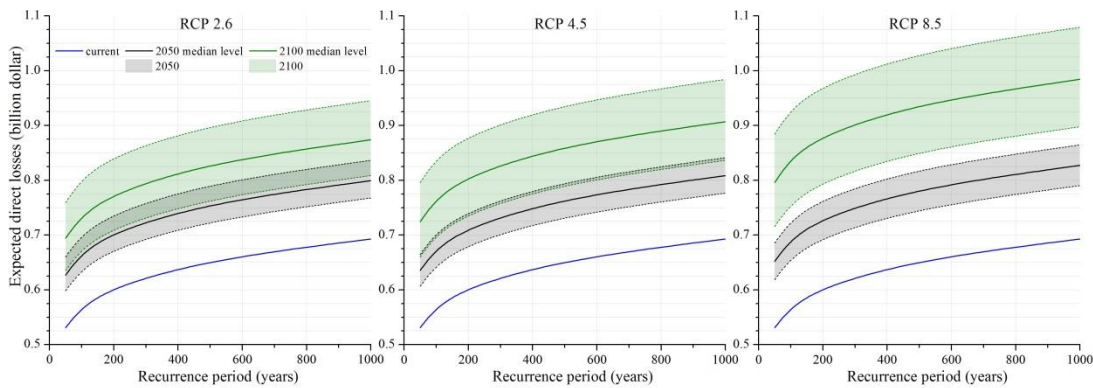
Flood damage does not only depend on inundated area and depth, but is related to the loss rates and values of exposed land-use types. The total expected direct flood losses would be exacerbated with sea-level rise (Fig. 4), but for current extreme floods, loss magnitudes are up to \$0.53 billion and \$0.69 billion for 50 to 1,000-year recurrence period CEWLs. Predictions for future extreme flood show an increase of more than 20% when the elevation of sea-level rise exceeds 0.3 m, however, the increase rates expand to beyond 40% given a 0.5 m sea-level rise. Indeed, by 2050, estimated losses under the RCP 2.6 scenario would be between \$0.6 billion and \$0.84 billion. These losses would be slightly increased by 2050 under the RCP 4.5 and 8.5 scenarios. Analyses show that expected direct losses would be more aggravated by the end of the century. By 2100, the smallest

205

206

current \$ value? No depreciation?

207 range of expected damage given the low degree RCP 2.6 scenario would be between \$0.63 billion
208 and \$0.81 billion. However, the maximum range of expected damage under the high degree RCP
209 8.5 scenario is predicted to be between \$0.88 billion and \$1.08 billion. It is worth noting that the
210 increase rates reach an average of 60% under the high degree of RCP 8.5 scenario with a 0.82 m
211 sea-level rise. The largest increase in predicted direct flood damage would be up to 29% in 2050
212 and 67% in 2100. Additive statistical information of future expected direct losses increase is
213 presented in Table S1(b). The losses for main land-use types under the high degree RCP 8.5 scenario
214 are shown in Table S2 and results indicated that residential land would be seriously affected by
215 extreme floods.
216



217
218
219

Fig. 4 Expected direct losses (billion, dollar) in 2050 and 2100 given different RCP scenarios.

No depreciation

220 3.3 Population and GDP affected by extreme water levels

221 With the rapid socio-economic development, population and GDP have distributed along the
222 coastline. Thus, a large proportion of both population and GDP are expected to be affected by
223 extreme floods. Affected population and GDP exposed to flooding would be higher with the
224 expansion of inundation area as a direct result of sea-level rise.

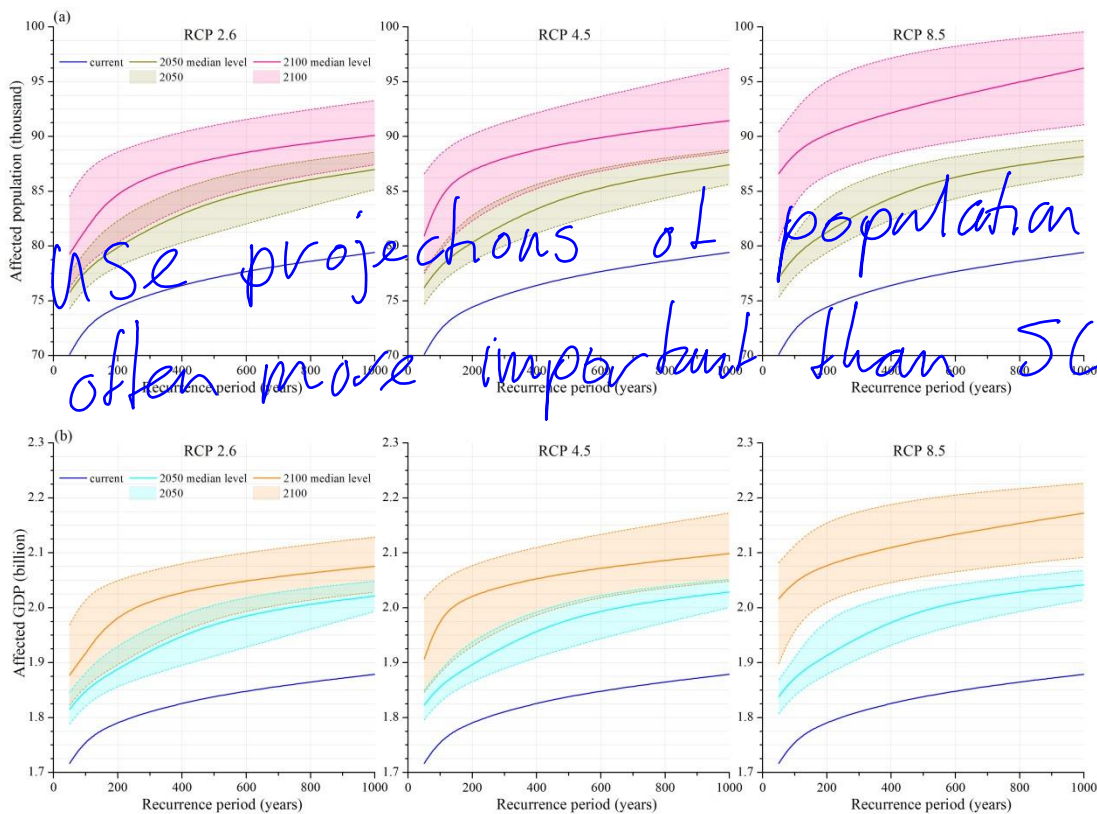
English

→ no more development after 2016?

225 The number of affected population under RCP scenarios of 2.6, 4.5, and 8.5 is shown as Fig.
226 5a. Expected population magnitudes, which would suffer from 50 to 1,000-year CEWLs, range
227 between about 70,000 and 79,000. In both 2050 and 2100, this increment is sharp with an enlarged
228 recurrence period and the maximum increment of affected population approaches 20,000 in 2050
229 and 30,000 in 2100. Considering the intermediate scenario of RCP 4.5, around 5.57% to 12.36%

230 more people would be confronted with the inundation risk in 2050, while the affected population
 231 would increase 9.52% to 23.53% in 2100. Detailed data of the increase in affected population are
 232 provided in Table S1(c).

233 Similarly, sea-level rise also leads to an increased GDP exposure; the scope of affected GDP is
 234 presented in Fig. 5b. In the case of no sea-level rise, the total GDP of Rongcheng City at risk from
 235 extreme floods would be between \$1.72 billion and \$1.88 billion. As inundated area increasing due
 236 to sea-level rise, the change in affected GDP is obvious. By 2100, projections for affected GDP
 237 increase from \$1.82 billion to \$2.23 billion. At the most extreme, under the high degree RCP 8.5
 238 scenario, affected GDP would increase by approximately 20% by the end of the century. Additional
 239 information about increases in affected GDP is given in Table S1(d).



240

241

242

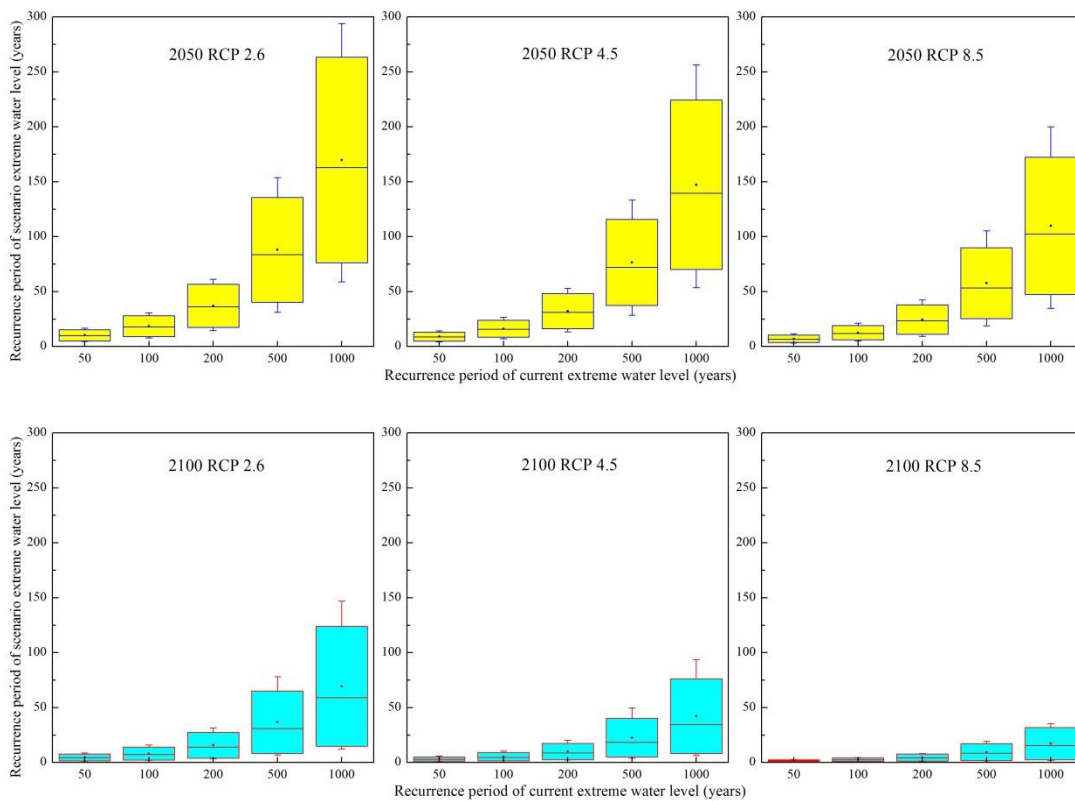
<Fig. 5 is here, thanks!>

243 Fig. 5 Affected population and GDP exposed to inundation in 2050 and 2100 under different RCP scenarios

244 **3.4 Variation of recurrence periods due to sea-level rise**

245 Refitting SEWLs combined CEWLs with future sea-level rise demonstrates that the recurrence
 246 periods would decrease sharply due to climate change (Fig. 6). Results suggest that, by 2050, the
 247 recurrence periods of extreme water levels would be shortened rapidly. For example, in 2050, the

248 100-year recurrence period for CEWL is likely to fall by eight years to 31-year (RCP 2.6), seven
 249 years to 26-year (RCP 4.5), and five-year to 21-year (RCP 8.5). In 2100, more seriously, CEWLs
 250 would be occurred more probably becoming common events under high degree RCP scenarios.
 251 Among the different RCP scenarios, the shrink of recurrence periods under RCP 8.5 is more
 252 significant than either RCP 2.6 or 4.5 scenarios. The worst case situation is that 1,000-year
 253 recurrence period of CEWL would be occurred every three years; once in a hundred year events are
 254 likely to become common, even occurring annually by the end of this century. Such recurrence
 255 periods shortening would significantly increase the flooding risk over coming decades.



256

257

258 **Fig. 6** Variation in recurrence periods of CEWLs and SEWLs in 2050 and 2100 under RCP 2.6, 4.5, and 8.5
 259 scenarios. In each RCP scenario, the variation in five representative recurrence periods of 50, 100, 200, 500 and
 260 1000-year is shown. And the yellow boxes stand for the recurrence intervals in 2050 and the blue boxes stand for
 261 the recurrence intervals in 2100. The data, presented the variation of recurrence periods, are just referred to
 262 Chengshantou and Shidao stations.

263

264 **4 Discussion**

265 Based on previous studies of individual hazard and vulnerability (e.g. Li and Li, 2011; Wahl et al.,
266 2011), the extreme risk of inundation was assessed by integrating both of them. In this study, the
267 risk increase induced to sea-level rise was highlighted by the comparison of current with future
268 extreme water levels. SEWLs were recalculated by combining CEWLs with sea-level rise in 2050
269 and 2100 under RCP 2.6, 4.5, and 8.5. The results showed that recurrence periods would be likely
270 reduced by more than 70% by 2050 and this decrease could even exceed 80% by 2100 given high
271 RCP scenarios. In a similar study, Nicholls (2002) reported that a 0.2 m rise in sea-level could
272 markedly reduce recurrence periods of extreme water levels and a ten-year high water event was
273 converted into a six-month event. Indeed, as recurrence periods shortened, low-lying coastal areas
274 would have a higher probability of flood destruction over the next few decades.

not clear

Do you find the same? What other case studies?

275 The continuous sea-level rise would enhance the potential destructive force of future flooding.
276 For example, the results demonstrated that the potential inundated area would be extended by 3%
277 to 11% in 2050 and by 5% to 20% in 2100. In contrast, sea-level rise increased the inundated area
278 exposed to a cyclonic storm surge in Bangladesh by 15% with a 0.3 m rise (Karim and Mimura,

use from to, or say the extend, now unclear

why?

→ stage - damage? or, more exposed?

279 2008). Results showed that residential land and farmland were more vulnerable to sea-level rise
280 coupled with a large potential inundated area and a high proportion of expected direct damage.
281 Residential land was under the biggest risk, according to projected SEWLs under future RCP
282 scenarios which expected direct losses would up to \$0.6 billion in 2050 and even exceed \$1.00
283 billion by 2100. To put these predicted losses into context, average annual flood losses of Tianjin
284 City was estimated to be as high as \$2.3 billion by 2050 (Hallegatte et al., 2013). It was predicted
285 that Shanghai, susceptible to high water levels, would be 46% underwater by 2100 with its seawalls
286 and levees submerged by rising sea-levels (Wang et al., 2012). A range of studies highlighted the
287 fact that many coastal cities, including San Francisco, would experience flooding in the near future
288 as a result of rising sea-level rather than heavy rainfall (Gaines, 2016). There was no doubt that
289 rising sea-levels would lead to a large number of people and property would be faced with flooding
290 risk, especially the fast growth of China's coastal cities (McGranahan et al., 2007; Smith, 2011).

291 Given the shortening of recurrence periods in future, property and assets exposed to extreme
292 floods would be more likely. For instance, results showed that under a RCP 8.5 scenario, an extreme

293 event that was possible to take place every 1,000 years and cause damage of \$0.7 billion would
294 occur about once every 50 years by 2050, even once every two years by 2100. Under these
295 circumstances, many people and industries at extreme risk from floods would have no choice but to
296 retreat from coastal regions. However, studies indicated that most coastal populations were
297 completely unprepared for an increasing risk of extreme floods, especially in developing countries
298 (Woodruff et al., 2013).

299 Although this study manifested that sea-level rise would significantly increase the flooding risk,
300 some uncertainties still remain. First, on account of spatial heterogeneity, regional sea-level rise
301 should be projected in the future work. The objective of this paper is just to reveal the scientific
302 question that the impact of sea-level rise under global warming on extreme floods so that the
303 projection of global mean sea-level rise was used for its availability, which is consist with Wu et al.,
304 (2016). Nevertheless, there is no obvious land subsidence for the regional crustal stability. Second,
305 the combination of climate and weather extremes, including storm surges, astronomical tides,
306 rainfall and sea-level rise need to be focused on as they underlie and amplify the extreme events as
307 well as generating extreme conditions (Leonard et al., 2014). Because the coastal regions of China
308 have a monsoonal climate, combining inundation risk assessment with consideration of rainfall is
309 particularly important (Bart et al., 2015; Wahl et al., 2015). Third, human activities, which impact
310 on socio-economic development and alter feedbacks from climate change, are the mainly driving
311 force of future inundation risk (Stevens et al., 2015) and should be focused in the next research.
312 Consequently, the deeper exploration aiming at these uncertainties would be undertaken.

313 **5 Conclusions**

314 This study assessed the inundation risk resulting from extreme water levels with future projections
315 for 2050 and 2100 under different RCP scenarios. Results demonstrated that continuous sea-level
316 rise would augment the inundation risk by shortening recurrence periods and increasing the expected
317 losses and potential effect. (1) Sea-level rise would make low-lying coastal regions more possible
318 to be exposed to flood because of the recurrence periods shortening of extreme water levels. (2)
319 Inundation risk would be increased by the increment of inundated area, direct damage, and affected
320 population and GDP. (3) The analysis presented that sea-level rise principally threatened the vertical

321 land-use types for human survival, especially residential land and farmland. (4) Projections showed
322 that inundation risk would continue to increase up to 2100 and would be the most serious under the
323 RCP 8.5 scenario. In summary, these results revealed that sea-level rise dramatically increased the
324 flooding risk. Effective mitigation and adaptation plans are needed to deal with the increasing
325 coastal inundation risk.

326 **Acknowledgements**

327 This research project was supported by the National Science and Technology Support Program of
328 China (Grant No. 2013BAK05B04), the National Natural Science Foundation of China (Grant No.
329 41301089) and the Clean Development Mechanism Funding Projects of China (Grant No. 2013034).
330 The authors also thanked Dr. Wenhui Kuang (IGSNRR, CAS) for providing the high-precision land-
331 use dataset of Rongcheng City.

332 **References**

- 333 Alfieri, L., Feyen, L., Dottori, F., and Bianchi, A.: Ensemble flood risk assessment in Europe under high end climate
334 scenarios, *Glob. Environ. Chang.*, 35, 199-212, 2015.
- 335 Bart van den, H., Erik van, M., Paul de, V., Klaas-Jan van, H., and Jan, G.: Analysis of a compounding surge and
336 precipitation event in the Netherlands, *Environ. Res. Lett.*, 10, 035001, 2015.
- 337 Bhuiyan, M. J. A. N., and Dutta, D.: Analysis of flood vulnerability and assessment of the impacts in coastal zones
338 of Bangladesh due to potential sea-level rise, *Nat. Hazards*, 61, 729-743, 2011.
- 339 Church, J. A., and White, N. J.: Sea-Level Rise from the Late 19th to the Early 21st Century, *Surv. Geophys.*, 32,
340 585-602, DOI 10.1007/s10712-011-9119-1, 2011.
- 341 Cooley, D., Nychka, D., and Naveau, P.: Bayesian spatial modeling of extreme precipitation return levels, *J. Am.*
342 *Stat. Assoc.*, 102, 824-840, 2007.
- 343 Dutton, A., Carlson, A., Long, A., Milne, G., Clark, P., DeConto, R., Horton, B., Rahmstorf, S., and Raymo, M.:
344 Sea-level rise due to polar ice-sheet mass loss during past warm periods, *Science*, 349, aaa4019, 2015.
- 345 Feng, A. Q., Gao, J. B., Wu, S. H., Liu, Y. H., He, X. J.: A review of storm surge disaster risk research and adaptation
346 in China under climate change (In Chinese), *Progress in Geography*, 35, 1411-1419, 2016.
- 347 Feng, X., and Tsimplis, M. N.: Sea level extremes at the coasts of China, *J. Geophys. Res.*, 119, 1593-1608, 2014.
- 348 Gaines, J. M.: Flooding: Water potential, *Nature*, 531, S54-S55, 10.1038/531S54a, 2016.
- 349 Guneralp, B., Guneralp, I., and Liu, Y.: Changing global patterns of urban exposure to flood and drought hazards,
350 *Glob. Environ. Chang.*, 31, 217-225, 2015.
- 351 Haigh, I., Wijeratne, E. M. S., MacPherson, L., Pattiaratchi, C., Mason, M., Crompton, R., and George, S.: Estimating
352 present day extreme water level exceedance probabilities around the coastline of Australia: tides, extra-tropical
353 storm surges and mean sea level, *Clim. Dyn.*, 42, 121-138, 10.1007/s00382-012-1652-1, 2014a.
- 354 Haigh, I. D., MacPherson, L. R., Mason, M. S., Wijeratne, E. M. S., Pattiaratchi, C. B., Crompton, R. P., and George,
355 S.: Estimating present day extreme water level exceedance probabilities around the coastline of Australia:

356 tropical cyclone-induced storm surges, *Clim. Dyn.*, 42, 139-157, 2014b.

357 Hallegatte, S., Green, C., Nicholls, R. J., and Corfee-Morlot, J.: Future flood losses in major coastal cities, *Nature*
358 *Clim. Change*, 3, 802-806, 10.1038/nclimate1979, 2013.

359 Hinkel, J., Lincke, D., Vafeidis, A. T., Perrette, M., Nicholls, R. J., Tol, R. S., Marzeion, B., Fettweis, X., Ionescu,
360 C., and Levermann, A.: Coastal flood damage and adaptation costs under 21st century sea-level rise, *Proc. Natl.*
361 *Acad. Sci. USA*, 111, 3292-3297, 2014.

362 Hirabayashi, Y., Mahendran, R., Koirala, S., Konoshima, L., Yamazaki, D., Watanabe, S., Kim, H., and Kanae, S.:
363 Global flood risk under climate change, *Nature Clim. Change*, 3, 816-821, 2013.

364 Holgate, S. J.: On the decadal rates of sea level change during the twentieth century, *Geophys. Res. Lett.*, 34, Art
365 L01602 Doi 10.1029/2006gl028492, 2007.

366 Hunter, J.: A simple technique for estimating an allowance for uncertain sea-level rise, *Clim. Chang.*, 113, 239-252,
367 2012.

368 IPCC: *Climate Change 2013: The physical science basis: Working group I contribution to the fifth assessment report*
369 *of the Intergovernmental Panel on Climate Change*, Cambridge University Press, 2013.

370 Karim, M. F., and Mimura, N.: Impacts of climate change and sea-level rise on cyclonic storm surge floods in
371 Bangladesh, *Glob. Environ. Chang.*, 18, 490-500, 2008.

372 Kirwan, M. L., and Megonigal, J. P.: Tidal wetland stability in the face of human impacts and sea-level rise, *Nature*,
373 504, 53-60, 2013.

374 Klerk, W. J., Winsemius, H. C., Verseveld, W. J. v., Bakker, A. M. R., and Diermanse, F. L. M.: The co-occurrence of
375 storm surges and extreme discharges within the Rhine–Meuse Delta, *Environ. Res. Lett.*, 10, 035005, 2015.

376 Kopp, R. E., Simons, F. J., Mitrovica, J. X., Maloof, A. C., and Oppenheimer, M.: A probabilistic assessment of sea
377 level variations within the last interglacial stage, *Geophys. J. Int.*, 193, 711-716, Doi 10.1093/Gji/Ggt029, 2013.

378 Leonard, M., Westra, S., Phatak, A., Lambert, M., van den Hurk, B., McInnes, K., Risbey, J., Schuster, S., Jakob, D.,
379 and Stafford-Smith, M.: A compound event framework for understanding extreme impacts, *Wires Clim. Change*,
380 5, 113-128, 10.1002/wcc.252, 2014.

381 Levermann, A., Clark, P. U., Marzeion, B., Milne, G. A., Pollard, D., Radic, V., and Robinson, A.: The
382 multimillennial sea-level commitment of global warming, *Proc. Natl. Acad. Sci. USA*, 110, 13745-13750, 2013.

383 Li, K., and Li, G. S.: Vulnerability assessment of storm surges in the coastal area of Guangdong Province, *Nat.*
384 *Hazards Earth Syst. Sci.*, 11, 2003-2010, 10.5194/nhess-11-2003-2011, 2011.

385 McGranahan, G., Balk, D., and Anderson, B.: The rising tide: assessing the risks of climate change and human
386 settlements in low elevation coastal zones, *Environment and urbanization*, 19, 17-37, 2007.

387 Mokrech, M., Nicholls, R. J., and Dawson, R. J.: Scenarios of future built environment for coastal risk assessment
388 of climate change using a GIS-based multicriteria analysis, *Environ. Plann. B*, 39, 120-136, Doi
389 10.1068/B36077, 2012.

390 Muis, S., Güneralp, B., Jongman, B., Aerts, J. C. J. H., and Ward, P. J.: Flood risk and adaptation strategies under
391 climate change and urban expansion: A probabilistic analysis using global data, *Sci. Total Environ.*, 538, 445-
392 457, 2015.

393 Neumann, B., Vafeidis, A. T., Zimmermann, J., and Nicholls, R. J.: Future Coastal Population Growth and Exposure
394 to Sea-Level Rise and Coastal Flooding - A Global Assessment, *Plos One*, 10, 10.1371/journal.pone.0118571,
395 2015.

396 Nicholls, R. J.: Analysis of global impacts of sea-level rise: a case study of flooding, *Phys. Chem. Earth, Parts A/B/C*,
397 27, 1455-1466, 2002.

398 Nicholls, R. J., and Cazenave, A.: Sea-Level Rise and Its Impact on Coastal Zones, *Science*, 328, 1517-1520,
399 10.1126/science.1185782, 2010.

400 Pugh, D.: Changing sea levels: effects of tides, weather and climate, Cambridge University Press, 2004.

401 Quinn, N., Lewis, M., Wadey, M. P., and Haigh, I. D.: Assessing the temporal variability in extreme storm-tide time
402 series for coastal flood risk assessment, *J. Geophys. Res.*, 119, 4983-4998, 10.1002/2014jc010197, 2014.

403 Ray, R. D., and Douglas, B. C.: Experiments in reconstructing twentieth-century sea levels, *Prog. Oceanogr.*, 91,
404 496-515, DOI 10.1016/j.pocean.2011.07.021, 2011.

405 Smith, K.: We are seven billion, *Nature Clim. Change*, 1, 331-335, 2011.

406 Stevens, A. J., Clarke, D., Nicholls, R. J., and Wadey, M. P.: Estimating the long-term historic evolution of exposure
407 to flooding of coastal populations, *Nat. Hazards Earth Syst. Sci.*, 15, 1215-1229, 10.5194/nhess-15-1215-2015,
408 2015.

409 Strauss, B. H., Ziemiński, R., Weiss, J. L., and Overpeck, J. T.: Tidally adjusted estimates of topographic
410 vulnerability to sea level rise and flooding for the contiguous United States, *Environ. Res. Lett.*, 7, 014033,
411 2012.

412 Syvitski, J. P., Kettner, A. J., Overeem, I., Hutton, E. W., Hannon, M. T., Brakenridge, G. R., Day, J., Vörösmarty,
413 C., Saito, Y., and Giosan, L.: Sinking deltas due to human activities, *Nat. Geosci.*, 2, 681-686, 2009.

414 Trenberth, K. E., Fasullo, J. T., and Shepherd, T. G.: Attribution of climate extreme events, *Nature Clim. Change*, 5,
415 725-730, 10.1038/nclimate2657, 2015.

416 Wahl, T., Muddersbach, C., and Jensen, J.: Assessing the hydrodynamic boundary conditions for risk analyses in
417 coastal areas: a stochastic storm surge model, *Nat. Hazards Earth Syst. Sci.*, 11, 2925-2939, DOI 10.5194/nhess-
418 11-2925-2011, 2011.

419 Wahl, T., Jain, S., Bender, J., Meyers, S. D., and Luther, M. E.: Increasing risk of compound flooding from storm
420 surge and rainfall for major US cities, *Nature Clim. Change*, 5, 1093-1097, 2015.

421 Wang, J., Gao, W., Xu, S., and Yu, L.: Evaluation of the combined risk of sea level rise, land subsidence, and storm
422 surges on the coastal areas of Shanghai, China, *Clim. Change*, 115, 537-558, 10.1007/s10584-012-0468-7, 2012.

423 Winsemius, H. C., Aerts, J. C. J. H., van Beek, L. P. H., Bierkens, M. F. P., Bouwman, A., Jongman, B., Kwadijk, J.
424 C. J., Ligtoet, W., Lucas, P. L., van Vuuren, D. P., and Ward, P. J.: Global drivers of future river flood risk,
425 *Nature Clim. Change*, 6, 381-385, 2016.

426 Woodruff, J. D., Irish, J. L., and Camargo, S. J.: Coastal flooding by tropical cyclones and sea-level rise, *Nature*,
427 504, 44-52, 10.1038/nature12855, 2013.

428 Wu, S. H., Feng, A. Q., Gao, J. B., Li, Y. Z., Wang, L.: Shortening the recurrence periods of extreme water levels
429 under future sea-level rise, *Stoch. Env. Res. Risk Assess.*, 2016. doi: 10.1007/s00477-016-1327-2.

430 Xu, L., He, Y., Huang, W., and Cui, S.: A multi-dimensional integrated approach to assess flood risks on a coastal
431 city, induced by sea-level rise and storm tides, *Environ. Res. Lett.*, 11, 014001, 2016.

432 Yang, S., Liu, X., and Liu, Q.: A storm surge projection and disaster risk assessment model for China coastal areas,
433 *Nat. Hazards*, 84, 649-667, 10.1007/s11069-016-2447-1, 2016.

434 Yin, J.: Study on the risk assessment of typhoon storm tide in China coastal area, Shanghai: East China Normal
435 University, 2011.

436 Yin, J., Yin, Z., Wang, J., and Xu, S.: National assessment of coastal vulnerability to sea-level rise for the Chinese
437 coast, *J. Coast. Conserv.*, 16, 123-133, 10.1007/s11852-012-0180-9, 2012.